ACS OMEGA

http://pubs.acs.org/journal/acsodf

Article

Experimental Investigation of the Attachment Performance between Coal Particle and Bubble

Qiming Zhuo, Wenli Liu,* Hongxiang Xu,* He Zhang, and Xiaopeng Sun

Cite This: *ACS Omega* 2021, 6, 7979−7987

Read Online

ACCESS | Metrics & More | Article Recommendations | Supporting Information

ABSTRACT: Attachment behavior is a key component of flotation and has a decisive influence on flotation performance, and the experiment research on the attachment between mineral particles and bubbles still needs further research. In this work, a particle−bubble attachment apparatus and multiple target tracking software were developed. Coal particles were used as the subjects, and the effect of particle properties on the attachment performance was studied from the perspective of the particle group. The particle−bubble attachment experiments indicated that the collision position had an effect on the attachment efficiency, and the attachment efficiency decreased with an increase in the collision angle. The efficiency-weighted attachment angle was proposed to quantitatively describe the attachment performance of coal samples. The efficiency-weighted attachment angle of low-density coal samples was greater than that of high-density coal samples. For particles with different sizes, the efficiency-weighted attachment angle of fine particles was greater than that of coarse particles. Furthermore, SDS weakened the attachment performance between coal particles and bubbles via adsorption on the bubble, and the efficiency-weighted attachment angle decreased as the concentration of the SDS solution increased. CTAB adsorbed on coal particles and bubbles, and the efficiency-weighted attachment angle first increased and then decreased with increasing CTAB concentration.

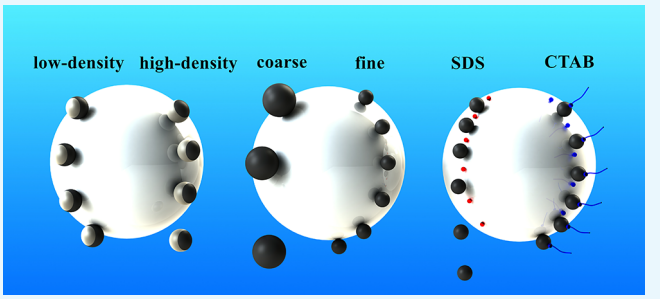

INTRODUCTION

Flotation in which bubbles are used as carriers to separate valuable minerals from ores according to the differences in particle surface properties is one of the most mature beneficiation methods for fine mineral particles.[1,2] In general, the particle−bubble interactions in flotation can be divided into three subprocesses: (i) collision between a particle and bubble, (ii) attachment of a particle and bubble and the rising of particle−bubble aggregates, and (iii) detachment of a particle from a bubble in the rising process.[3,4] The collision process is mainly affected by the particle size, bubble size, and fluid state in the flotation cell. This is the first step to capture the target mineral, but there is no selectivity.[5] After the collision, the thin liquid film between particles and bubbles starts to thin via surface force until the liquid film ruptures, forming stable particle−bubble aggregates.[6] The attachment process is closely related to the surface hydrophobicity of particles, and the hydrophobic particles are more easily captured by bubbles; therefore, the attachment process is crucial for the selectivity of flotation.[7−9]

In terms of the attachment process between coal particles and bubbles, the investigation methods can be divided into thermodynamic and dynamic methods. The thermodynamic method estimates the particle−bubble attachment behavior (whether it happens and how easy it is) by measuring the change in Gibbs energy during the coal particle and bubble attachment process.[10] From the viewpoint of thermodynamics, once the contact angle of the particle is greater than 0, the particles have a tendency to attach to the bubbles, and the stronger the particle hydrophobicity, the stronger is the tendency to attach.[11] However, owing to the neglect of the liquid film drainage process and the energy barrier,[12] it is difficult to accurately analyze the attachment behavior between coal particles and bubbles only from the viewpoint of thermodynamics.

Compared with the thermodynamic method, the dynamic method is based on the specific steps where particles attach to bubbles.[13] The dynamic method focuses on the induction time,[14,15] surface force,[16−19] attachment efficiency,[20−22] and relative motion between particles and bubbles.[23−25] In recent years, the development of high-speed photography technology has made the visualization study of the particle−bubble attachment process popular.[26−28] Wang[20] et al. developed a particle−bubble attachment apparatus and recorded the

Received: August 24, 2020
Accepted: March 9, 2021
Published: March 18, 2021

https://doi.org/10.1021/acsomega.0c04093
ACS Omega 2021, 6, 7979−7987

attachment process of glass beads with different hydrophobicities on a stationary bubble. Their work indicated that hydrophilic particles only slid on the top half of the bubble without an attachment, and the hydrophobic particle slid over the entire bubble surface without detaching from the bubble. The work of Verrelli[7] indicated that the trajectories and velocities of glass beads exhibit substantial asymmetry about the equatorial plane of the bubble and believed that the mobility of the bubble surface was at an intermediate level between "full slip" and "no slip." Nguyen[29] found that hydrophobic glass beads jumped toward the bubble after a period of sliding and were subsequently found to have an attachment. Furthermore, certain research results proved that the attachment behavior was influenced by the collision position, shape of the particle, and presence of surfactants.[30−32]

Studies have shown that the attachment process plays a major role in mineral flotation, and several factors can affect the attachment behavior. However, experimental research on the attachment behavior between mineral particles and bubbles has been inadequate. In this study, a particle−bubble attachment apparatus was developed to further investigate the particle−bubble attachment behavior, and coal particles were taken as the research subject. The effects of particle density, particle size, and different surfactants on the attachment performance were explored using visual and quantitative approaches.

RESULTS AND DISCUSSION

Changes in Particle Density. In mineral flotation, particles with different densities generally exhibit different flotation responses. In this section, six coal samples with different densities (−1.3, 1.3−1.4, 1.4−1.5, 1.5−1.6, 1.6−1.7, and +1.7 g/cm^3) at the same particle size (0.15−0.10 mm) were used to study the effect of particle density on the attachment performance. Figure 1 depicts the attachment efficiency of particles with different densities at various collision angles. The collision angle is the angle between the connection of the collision point to the bubble center and the vertical direction, and the detailed calculation method was shown in our previous work.[21]

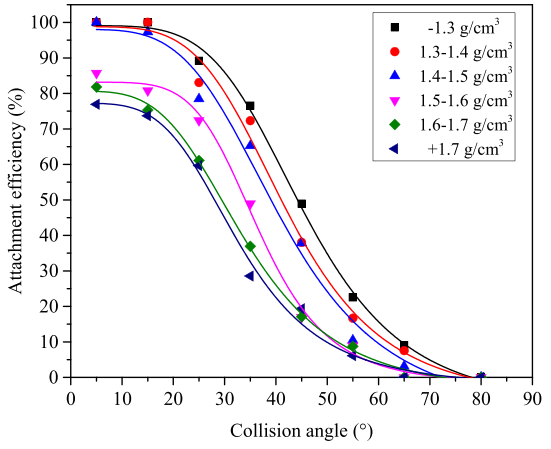

Figure 1. Attachment efficiency of coal samples with different densities.

The results shown in Figure 1 indicate that the attachment efficiency decreased with an increase in the collision angle. Taking the coal sample with a density of −1.3 g/cm^3 as an example, the attachment efficiency was approximately 100% when the collision angle was less than 20°. As the collision angle increased, the attachment efficiency decreased rapidly, and the coal particles had difficulty in attaching to the bubbles when the collision angle was greater than 60°. Furthermore, the attachment efficiency of low-density coal particles was greater than that of high-density particles at the same collision angle.

Our previous studies have demonstrated that particle collision velocity (the velocity measured in the experiment when the particle collided with the bubble) increased with an increase in collision angle.[21,33] Therefore, if the particle collides with the bubble at a small collision angle, the particle velocity at the collision point is very small, which means that there is a big loss in the particle's kinetic energy. This kinetic energy has been used to drain the thin liquid film. As the collision angle increases, the particle velocity at the collision point increases gradually, which means that the particle's ability to puncture the thin liquid film decreases. In addition, the increase in collision angle shortened the sliding distance of coal particles on the surface of the bubble, resulting in a reduction in the contact time. Therefore, the three-phase contact line was hardly formed, and the coal sample attachment efficiency decreased as the collision angle increased.

The "efficiency-weighted attachment angle" was introduced to quantitatively compare the attachment performance between coal samples. The idea of obtaining the efficiency-weighted attachment angle is as follows. After the experiment, eight data points (each point represents the attachment efficiency in different collision intervals) were obtained. Then, some nonlinear curve modes were used to fit these data according to the trend of points, and it was found that the logistic model can fit the data points very well. The value of adjusted R square can reach 0.99, and the fitting error of Figure 1 is shown in Table S1. Then, the complicated Gauss−Legendre numerical integration was adopted to calculate the area enclosed by the curve (a program was developed in Matlab and realized the automatic calculation). At last, we defined this value as the efficiency-weighted attachment angle to reflect the attachment performance of coal samples and bubbles. The results are presented in Figure 2.

The efficiency-weighted attachment angle of the coal samples decreased with an increase in particle density,

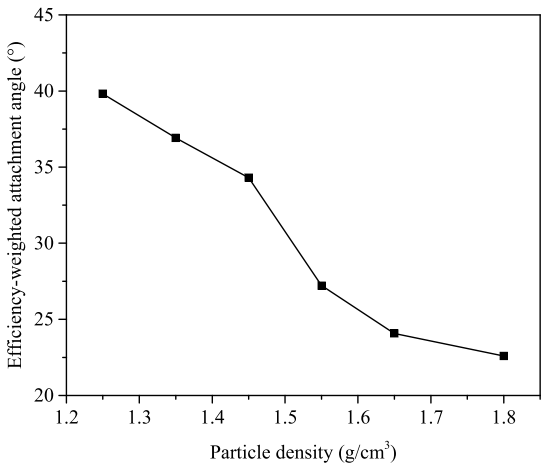

Figure 2. Efficiency-weighted attachment angle of coal samples with different densities.

https://doi.org/10.1021/acsomega.0c04093
ACS Omega 2021, 6, 7979−7987

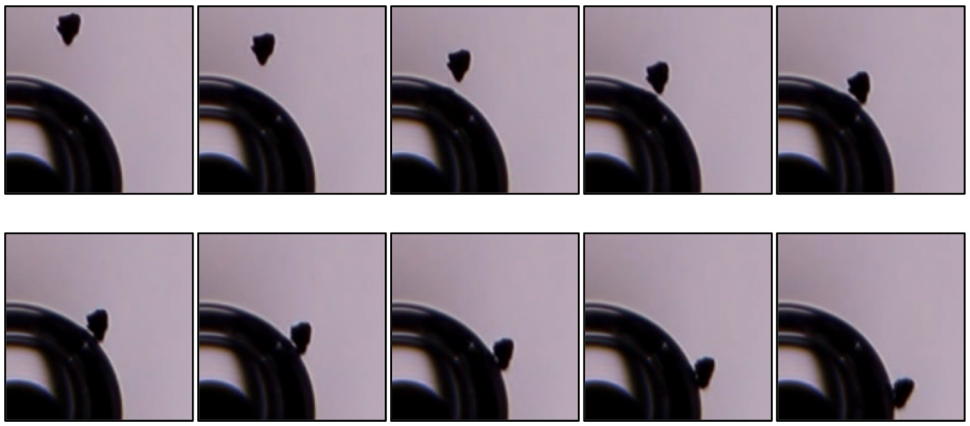

Figure 3. Movement of particles near the bubble.

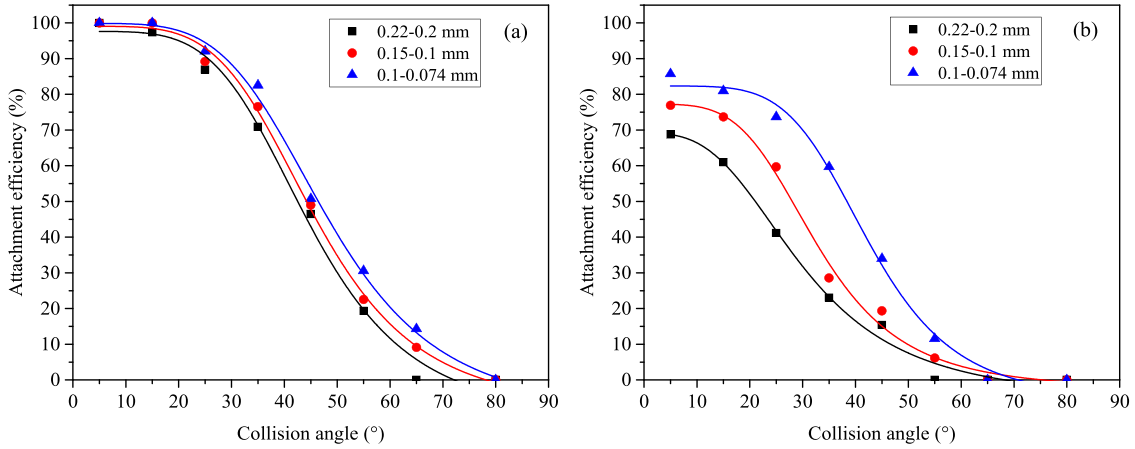

Figure 4. Attachment efficiency of coal samples with different particle sizes of (a) −1.3 and (b) +1.7 g/cm^3.

indicating that the attachment performance was poor when the particle density was high, which is consistent with the flotation theory. According to the analysis, the density difference between coal samples was related to the ratio of organic and inorganic components in the coal. The density of the organic component was lower than that of the inorganic component, and the organic component had higher hydrophobicity. The density of the coal particles decreased as the proportion of organic component increased. The surface force between the organic component and bubbles promoted the thinning and rupture of the water film, and coal particles were more likely to attach to the bubbles. Moreover, the observation of the particle movement indicated that the contact between particles and bubbles started from a small part (see Figure 3). If the components of the particles were organic at the contact part, the particles easily attached to the bubbles. The proportion of the organic component increased as the density of the coal sample decreased, resulting in an increase in the contact probability of the organic component with bubbles. Therefore, the attachment performance of low-density coal samples was greater than that of high-density coal samples.

Changes in Particle Size. Particle size plays a vital role in flotation and has a significant effect on the attachment between particles and bubbles. In this section, coal samples with different particle sizes (0.22−0.20, 0.15−0.10, and 0.10−0.074 mm) at low density (−1.3 g/cm^3) and high density (+1.7 g/cm^3) were used to study the effect of particle size on the attachment performance. The attachment efficiency results are presented in Figure 4.

As illustrated in Figure 4, in the low-density coal samples, the attachment efficiency of the coal sample with a fine particle size was greater than that of the coal sample with a coarse particle size at the same collision angle, but the distinction is not obvious. When the density of the coal sample increased to +1.7 g/cm^3, the trend of the attachment efficiency was similar to that of the low-density coal samples; that is, the attachment efficiency decreased with an increase in the particle size. The difference is that when the density of the coal particles was higher, the attachment efficiency of fine particles was much greater than that of coarse particles. Figure 5 presents a visual representation of this phenomenon.

In Figure 5, the efficiency-weighted attachment angle of the low-density samples was greater than that of the high-density samples, and the efficiency-weighted attachment angle decreased with an increase in particle size at the same density. Furthermore, the efficiency-weighted attachment angle of the high-density sample decreased faster than that of the low-density sample. Therefore, the high-density coal samples still have a high efficiency-weighted attachment angle when the particle size is small. For instance, when the particle size is 0.1−0.074 mm and the density is +1.7 g/cm^3, the efficiency-weighted attachment angle is 30.39° (point B). Although it is still smaller than the efficiency-weighted attachment angle of the low-density sample (point A), the difference is not large compared with the coarse sample, as marked in the figure. This

https://doi.org/10.1021/acsomega.0c04093
ACS Omega 2021, 6, 7979−7987

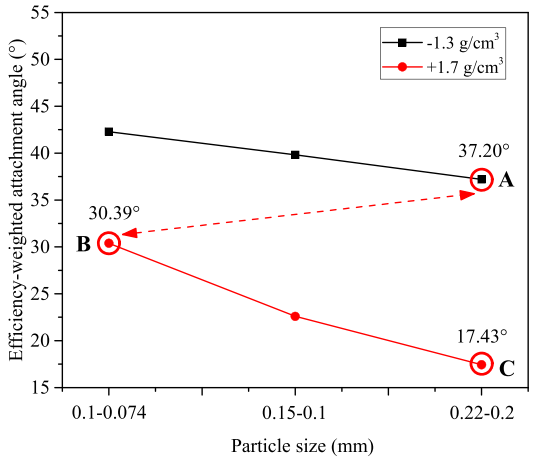

Figure 5. Efficiency-weighted attachment angle of coal samples with different particle sizes.

indicates that the high-density fine particles are also easy to attach to the bubbles. Furthermore, the efficiency-weighted attachment angle of high-density coarse particles is very small (17.43°, point C), which means the high-density coarse particles is difficult to attach to the bubbles. Moreover, the ash content of the coal particle increases with the increase in the coal sample density. Therefore, it is thought that this result provides an explanation for how fine particles with a high ash content cause pollution in the flotation concentrate. The attachment efficiency of fine particles is much greater than that of coarse particles as the coal particle density increases, resulting in finer coal particles with a higher ash content entering the flotation concentrate than coarse particles.

The analysis indicated that the hydrophobicity of coal particles was similar to each other at the same density, but the terminal velocity of particles increased as the particle size increased, resulting in a high collision velocity with bubbles and a decrease in contact time. Furthermore, certain research results indicated that an increase in the particle size leads to a longer induction time.[3] For instance, Ye[35] used an electronic induction timer to measure the induction time of five different coal samples, and the results show that the induction time of all samples increases as the size increases, which proved that the attachment performance of fine particles is greater than that of coarse particles. Therefore, the efficiency-weighted attachment angle of coarse particles is smaller than that of fine particles. In terms of coarse particles with low density, the strong hydrophobicity of particles enabled the particles to pierce the thin liquid film quickly and complete the attachment process. This result also indicates that the attachment behavior between particles and bubbles mainly depends on the hydrophobicity of the particle surface, and increasing the particle velocity cannot effectively improve the attachment efficiency.

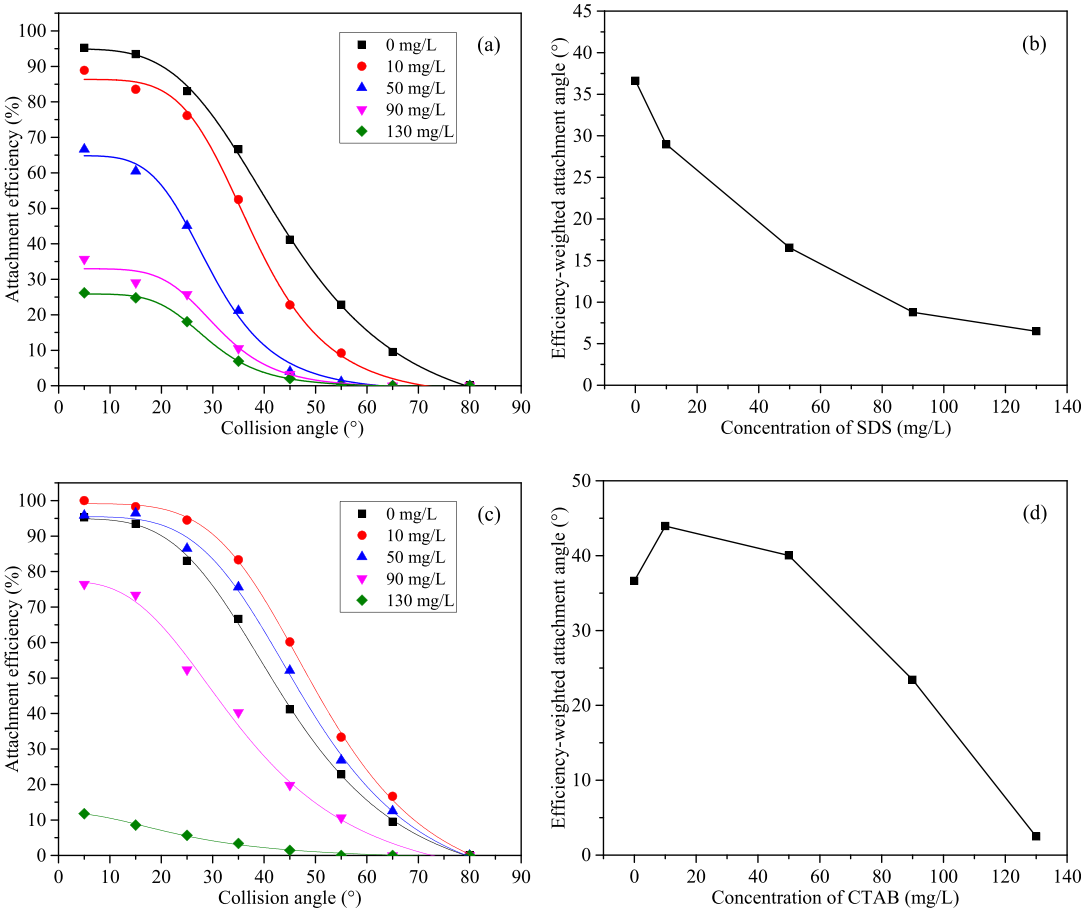

Figure 6. Attachment performance of coal samples in surfactant solutions: (a) attachment efficiency in the SDS solution, (b) efficiency-weighted attachment angle in the SDS solution, (c) attachment efficiency in the CTAB solution, and (d) efficiency-weighted attachment angle in the CTAB solution.

https://doi.org/10.1021/acsomega.0c04093
ACS Omega 2021, 6, 7979−7987

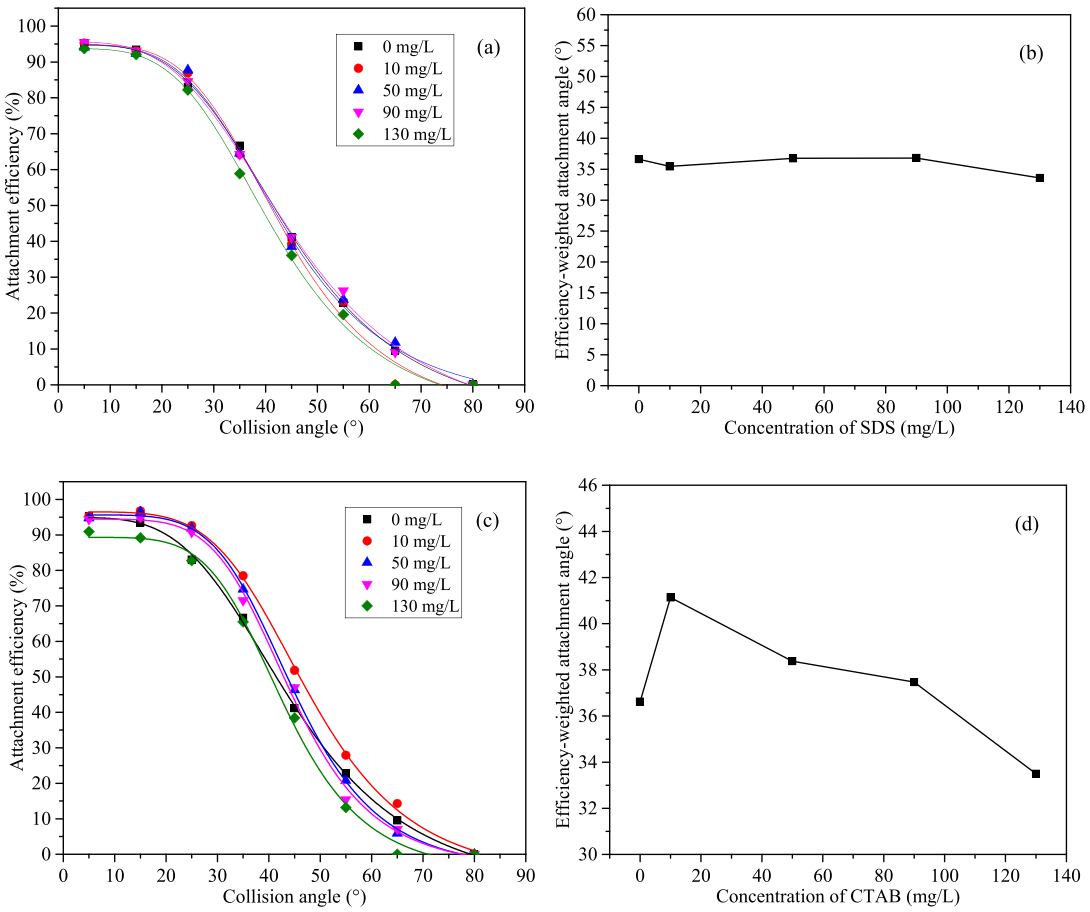

Figure 7. Attachment performance of coal samples when the surfactant is adsorbed on the surface of the coal particles: (a) attachment efficiency in the SDS solution, (b) efficiency-weighted attachment angle in the SDS solution, (c) attachment efficiency in the CTAB solution, and (d) efficiency-weighted attachment angle in the CTAB solution.

Effect of Surfactants on the Attachment Performance. *Surfactants Act on Coal Particles and Bubbles.* The experiments in Sections 2.1 and 2.2 were conducted in deionized water. However, in the actual flotation process, surfactants are generally added to the flotation cell to adjust the surface properties of the mineral particles. In this section, two typical surfactants (SDS, anionic surfactant; CTAB, cationic surfactant) were selected to study the effect of surfactants on the attachment performance between coal particles and bubbles, and the concentrations of the surfactant solutions were 10, 50, 90, and 130 mg/L. In the first part of the experiment, surfactants were added to a beaker and water tank to introduce surfactants into the environment where the particles and bubbles are located. In addition, coal samples with particle sizes of 0.10−0.074 mm and middle densities of 1.4−1.5 g/cm^3 were employed. The experimental results are summarized in Figure 6.

As shown in the figure, the attachment efficiency of coal samples in the SDS solution was lower than that of samples in deionized water at the same collision angle, and the efficiency-weighted attachment angle decreased as the concentration of the SDS solution increased, indicating that SDS weakened the attachment performance of the coal particles. For the CTAB solution, when the solution concentrations were 10 and 50 mg/L, the attachment efficiency of the coal samples was greater than the attachment efficiency in deionized water at the same collision angle, and the efficiency-weighted attachment angle decreased with the increasing solution concentration. The coal particles in the SDS solution and CTAB solution had difficulty adhering to the bubbles when the concentration of the solution was very high. For example, the efficiency-weighted attachment angle was only 2.48° when the CTAB concentration reached 130 mg/L.

The molecular structure of SDS was composed of polar (hydrophilic) and nonpolar (hydrophobic) groups. After adsorption on the bubble, SDS can effectively reduce the interfacial tension and the interface Gibbs energy. After the surfactant is adsorbed on the bubble surface, its nonpolar group is inserted into the bubble, and the polar group is inserted into the water. Surfactants are aligned on the bubble surface to form a protective film. In addition, due to the interaction between the polar groups and water molecules, a hydration layer is formed on the bubble surface, making the bubbles have a certain mechanical strength to resist the effects of external forces. Therefore, the adsorption of SDS on the gas−liquid interface will reduce the hydrophobicity of the bubbles, thereby reducing the attachment efficiency of the coal particles. Moreover, this result was consistent with the study of Preuss,[34] who measured the force between hydrophobic glass beads and bubbles in the SDS solution via atomic force microscopy. Their results indicated that glass beads need to overcome a certain resistance before attaching to the bubbles, and the resistance increased with an increase in the SDS concentration.

https://doi.org/10.1021/acsomega.0c04093
ACS Omega 2021, 6, 7979−7987

When the surfactant was CTAB, it produced positively charged groups after dissolution in water. This group would adsorb on the coal particles, which has a negative electron surface under electrostatic force, resulting in an increase in the coal particle hydrophobicity and attachment efficiency. In addition, CTAB was also adsorbed at the gas−liquid interface, reducing the hydrophobicity of the bubbles. As a result of the abovementioned factor, the efficiency-weighted attachment angle first increased and then decreased with an increase in the concentration of CTAB.

Surfactants Only Act on Coal Particles. The above experiment demonstrates that the type and concentration of surfactants affect the attachment performance of coal particles. SDS weakened the attachment performance of coal particles, and a small amount of CTAB strengthened their attachment performance. In those experiments, the coal particles and bubbles were in the same solution environment, that is, the surfactants acted on both the surface of the coal particles and bubbles. In the subsequent experiment, the surface of the coal particles was first modified with surfactants in a beaker, then transferred to the water tank, which contained deionized water. Therefore, it can be considered that the coal particles and bubbles were in two different solution environments, to some extent, and surfactants were only adsorbed on the surface of the coal particles. The attachment results are presented in Figure 7.

The efficiency-weighted attachment angle of coal samples remains stable at each SDS concentration, indicating that SDS has little effect on the coal particles' attachment performance. According to the analysis, SDS is an anionic surfactant, which is negatively charged after being dissolved in water; thus, it cannot be effectively adsorbed on the surface of coal particles due to electrostatic repulsion. In addition, the property of the bubble surface has not been altered. Based on the results presented in Figures 6 and 7, it can be concluded that SDS cannot be adsorbed on the coal particle surfaces, and SDS weakens the attachment performance between coal particles and bubbles via adsorption on the bubble.

When coal particles were in the CTAB solution, the change process was similar to the situation in Figure 8; the efficiency-weighted attachment angle first increased and then decreased with increasing CTAB concentration. When the concentration of CTAB solution increased from 0 to 10 mg/L, the efficiency-weighted attachment angle increased from 36.62 to 41.14°, indicating that the hydrophobicity of the coal particles was strengthened. As the concentration of CTAB continued to increase, the efficiency-weighted attachment angle began to decrease and remained greater than the efficiency-weighted attachment angle in deionized water until the concentration reached 90 mg/L, which was different from the situation in Figure 6.

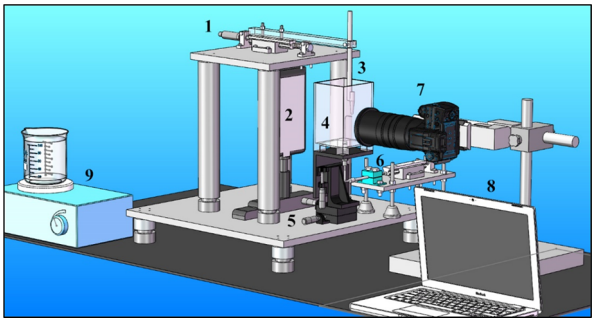

Figure 8. Schematic of the experimental apparatus (1) funnel micromoving device, (2) LED array light source, (3) feeding funnel, (4) water tank, (5) bubble micromoving device, (6) bubble-generating device, (7) camera, and (8) computer.

It was found that CTAB enhanced the hydrophobicity of coal particles after adsorbing on the particles, leading to an improvement in the efficiency-weighted attachment angle. As the concentration increased, a bilayer of CTAB formed at the solid−liquid interface, and the hydrophilic group faced outward. This caused a decrease in the hydrophobicity of the coal particles, making it difficult for the coal particles to attach to the bubbles. The coverage of the bilayer increased with increasing CTAB concentration. As a result, the efficiency-weighted attachment angle decreased with increasing CTAB concentration.

Based on the results in Figures 6 and 7, after dissolution in water, CTAB was adsorbed on the surface of coal particles and enhanced the hydrophobicity of the coal particles. The adsorption of the bilayer occurred on the surface of the coal particles as the CTAB concentration increased, leading to an increase in the hydrophobicity of the coal particles and efficiency-weighted attachment angle. Moreover, when CTAB adsorbed on the bubble, it weakened the hydrophobicity of the bubble and reduced the efficiency-weighted attachment angle.

CONCLUSIONS

Attachment behavior plays a critical role in flotation, and many factors can affect the attachment performance. A particle−bubble attachment apparatus and multiple target tracking software were developed to study coal particles with different properties attaching to bubbles. The entire particle−bubble attachment process was recorded and analyzed using self-developed software, and the effect of particle properties on the attachment performance was studied from the viewpoint of the particle group. The following conclusions can be drawn from our experiments:

1. In the case of the same coal sample, the attachment efficiency of coal particles decreased with an increase in the collision angle, which was caused by the increase in the collision velocity and decrease in the sliding distance.
2. The attachment performance of low-density coal samples were greater than that of high-density coal samples; higher organic component content in low-density coal samples increase the contact probability between the organic component and bubbles.
3. The efficiency-weighted attachment angle of fine particles was greater than that of coarse particles, but the distinction of efficiency-weighted attachment angle is complicated between coarse particles and fine particles. The efficiency-weighted attachment angle of fine particles was much greater than that of coarse particles when the density of coal particles was higher.
4. SDS weakened the attachment performance between coal particles and bubbles via adsorption on the bubble, and the efficiency-weighted attachment angle decreased as the concentration of the SDS solution increased.
5. After CTAB was adsorbed on coal particles and bubbles, a bilayer of CTAB would form as the solution concentration increased. This resulted in the efficiency-weighted attachment angle first increasing and then decreasing with the increasing CTAB concentration.

https://doi.org/10.1021/acsomega.0c04093
ACS Omega 2021, 6, 7979−7987

Table 1. Result of Proximate Analysis and Elemental Analysis

	proximate analysis/%				elemental analysis/%				
coal type	M_{ad}	A_{ad}	V_{ad}	Fc_{ad}	C	H	O	N	S
coking coal	0.39	20.56	23.37	55.68	86.13	5.35	5.51	1.34	1.67

MATERIALS AND METHODS

Coal Samples and Reagents. The coal sample was obtained from the Gongwusu mining area in Inner Mongolia, and the proximate analysis and elemental analysis of the coal sample (air dried) are summarized in Table 1.

The coal sample preparation approach is as follows: first, wet sieving was used to obtain samples with different particle sizes, and three groups of coal samples (0.22−0.2, 0.15−0.10, and 0.10−0.074 mm) were taken for further experiment. Second, the float−sink method was used to acquire coal samples with different densities (−1.3, 1.3−1.4, 1.4−1.5, 1.5−1.6, 1.6−1.7, and +1.7 g/cm^3), and 18 groups of coal samples were obtained. Analytical grade SDS (sodium dodecyl sulfate) and CTAB (hexadecyl trimethyl ammonium bromide) purchased from Aladdin Biochemistry Technology Company were used as surfactants. The aqueous solutions of these surfactants with desired concentrations were prepared through dissolution in deionized water (conductivity of 0.25 μS/cm). In addition, the terminal velocity of coal samples used in the experiment is shown in Table S8.

Particle−Bubble Attachment Apparatus. The particle−bubble attachment apparatus (see Figure 8) was developed based on previous studies[36,37] and was used to measure the attachment behavior between particles and bubbles. The bubble was generated using a gastight microsyringe, which was connected to a screw micrometer to ensure precise control of the bubble diameter. In addition, a stainless steel needle was hydrophobized using a chemical etching method (hydrochloric acid and 1*H*,1*H*,2*H*,2*H*-perfluorooctyltrichlorosilane) to attach the bubbles strongly. The bubble micromoving device was used to regulate the position of the bubble, and the moving accuracy was 0.01 mm. The coal samples used in the experiment were dispersed in a beaker via a magnetic stirrer, and the particles were transferred to the water tank using a pipette. Then, the coal particles fell into the feeding funnel under the action of gravity and collided with the bubble. Furthermore, the collision position was adjusted by controlling the feeding funnel and bubble micromoving device so that particles can collide with the bubbles at different collision angles. An LED array light source (Nangguang, CN-T96) was used to illuminate the water tank, which was composed of 8 × 12 LED lamp beads. The brightness of the lamp was 1672 lm, and the power of the lamp was 20 W. A camera was placed perpendicular to the water tank and focused on the bubble surface. In order to magnify the particles and show more detail, microphotography was used in this study. The depth of field was about 0.1 mm, and the magnification of the lenses was 10×. In addition, the shutter speed of the camera was 1/500 s, the frame rate was 50 Hz, and the resolution was 1280 × 720. The entire attachment process was recorded using this camera and monitored on a computer in real time. The collision and attachment processes were analyzed via a self-developed program, which allows accurate determination of the bubble and particle sizes, particle trajectories, particle velocity, and collision point between particles and bubbles. The experiment for each coal sample was approximately 5 h, and the number of successfully attached particles was approximately 1000 to ensure the accuracy of the experimental results. Furthermore, we will keep a close observation on the interaction process between particles and bubbles on the computer in the experiment. When about 15 particles are attached to the bubble, the bubble will be blown away, and a new bubble will be regenerated, and each experiment will consume approximately 90 bubbles. Moreover, the diameter of the bubble in this study was 1 ± 0.1 mm.

Experimental Data Processing. After a coal particle collided with a bubble, it would slide along the bubble surface. If the particle pierced the water film and formed a three-phase contact line between the particle and bubble by means of surface force, it would attach to the bubble; otherwise, it would detach from the bubble surface. These two situations are presented in Figure 9. To intuitively reflect the movement

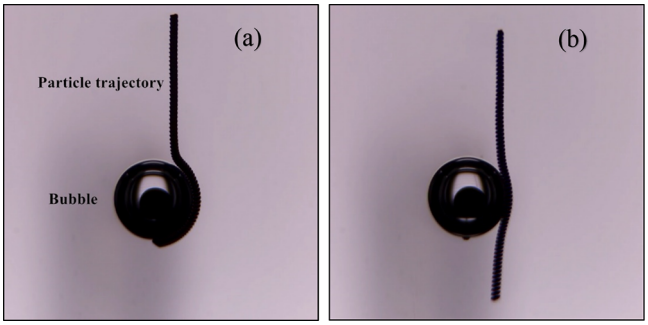

Figure 9. Photograph of the coal particle trajectory (a) particle colliding and attaching to the bubble and (b) particle colliding and detaching from the bubble.

process of particles, the photograph positions of each particle at different times were merged into one photograph. In addition, if the particle moves in front of or behind the bubble, the particle's trajectory will be interrupted by the bubble and cannot be observed in the camera. Therefore, this part of particles will be removed in the data processing, and only the particles whose trajectory is clearly visible will be retained.

The attachment efficiency is considered to characterize the attachment performance of the coal particles, which is obtained as the ratio of the attached particles to the total particles at a certain position. The attachment efficiency is calculated as follows:

$$E_a = \frac{N_a}{N_t} \quad (1)$$

where, N_a is the number of particles that do attach to bubbles; and N_t is the number of particles that collided with bubbles in the experiment. The counting of particle attachment was a very tedious task subject to human factors. Therefore, multiple target tracking software was developed to track all particles and extract useful parameters to determine whether particles and bubbles have attached. The principles for the implementation of this software were presented in our previous study.[33] Furthermore, certain research results indicated that the

https://doi.org/10.1021/acsomega.0c04093
ACS Omega 2021, 6, 7979−7987

collision angle has a significant effect on the attachment behavior between particles and bubbles; thus, the bubble surface was divided into 8 intervals according to the collision angle, and the attachment efficiency in each interval was calculated. In addition, when the collision angle was greater than 70°, the number of particles that can collide with bubbles was very small.[3] Therefore, these two intervals were merged into one interval to increase the accuracy of the results.

■ ASSOCIATED CONTENT

Supporting Information

The Supporting Information is available free of charge at https://pubs.acs.org/doi/10.1021/acsomega.0c04093.

Details of the attachment efficiency curve simulation result (Figure 1, Figure 4a,b, Figure 6a,c, and Figure 7a,c) (Tables S1-S7) and the terminal velocity of coal samples (Table S8) (PDF)

■ AUTHOR INFORMATION

Corresponding Authors

Wenli Liu − *School of Chemical and Environmental Engineering, China University of Mining & Technology (Beijing), Beijing 100083, China*; Phone: +86 13910724272; Email: liuwenli08@163.com

Hongxiang Xu − *School of Chemical and Environmental Engineering, China University of Mining & Technology (Beijing), Beijing 100083, China*; orcid.org/0000-0002-6280-3736; Phone: +86 13051886977; Email: xuhongxiang001@163.com

Authors

Qiming Zhuo − *School of Chemical and Environmental Engineering and College of Geoscience and Survey Engineering, China University of Mining & Technology (Beijing), Beijing 100083, China; State Key Laboratory of Mineral Processing, Beijing General Research Institute of Mining & Metallurgy, Beijing 102600, China*; orcid.org/0000-0001-7029-7549

He Zhang − *School of Mining Engineering, Heilongjiang University of Science and Technology, Heilongjiang 150080, China*; orcid.org/0000-0002-1750-4884

Xiaopeng Sun − *School of Chemical and Environmental Engineering, China University of Mining & Technology (Beijing), Beijing 100083, China*

Complete contact information is available at: https://pubs.acs.org/10.1021/acsomega.0c04093

Notes

The authors declare no competing financial interest.

■ ACKNOWLEDGMENTS

This research was funded by the National Natural Science Foundation of China (no. 51974324) and the Open Foundation of State Key Laboratory of Mineral Processing (no. BGRIMM-KJSKL-2020-22).

■ NOTATIONS

M_{ad} moisture of a coal sample under air drying
A_{ad} ash content of a coal sample under air drying
V_{ad} volatile component of a coal sample under air drying
Fc_{ad} fixed carbon of a coal sample under air drying
E_a attachment efficiency
N_a number of particles that do attach to bubbles
N_t number of particles that collide with bubbles in the experiment

■ REFERENCES

(1) Rao, F.; Liu, Q. Froth Treatment in Athabasca Oil Sands Bitumen Recovery Process: A Review. *Energy Fuels* **2013**, *27*, 7199−7207.

(2) Li, Y.; Chen, J.; Shen, L. Flotation Behaviors of Coal Particles and Mineral Particles of Different Size Ranges in Coal Reverse Flotation. *Energy Fuels* **2016**, *30*, 9933−9938.

(3) Albijanic, B.; Ozdemir, O.; Nguyen, A. V.; Bradshaw, D. A review of induction and attachment times of wetting thin films between air bubbles and particles and its relevance in the separation of particles by flotation. *Adv. Colloid Interface Sci.* **2010**, *159*, 1−21.

(4) Albijanic, B.; Ozdemir, O.; Hampton, M. A.; Nguyen, P. T.; Nguyen, A. V.; Bradshaw, D. Fundamental aspects of bubble-particle attachment mechanism in flotation separation. *Miner. Eng.* **2014**, *65*, 187−195.

(5) Dai, Z.; Fornasiero, D.; Ralston, J. Particle-bubble collision models-a review. *Adv. Colloid Interface Sci.* **2000**, *85*, 231−256.

(6) Xing, Y.; Gui, X.; Pan, L.; Pinchasik, B.-E.; Cao, Y.; Liu, J.; Kappl, M.; Butt, H.-J. Recent experimental advances for understanding bubble-particle attachment in flotation. *Adv. Colloid Interface Sci.* **2017**, *246*, 105−132.

(7) Verrelli, D. I.; Koh, P. T. L.; Nguyen, A. V. Particle-bubble interaction and attachment in flotation. *Chem. Eng. Sci.* **2011**, *66*, 5910−5921.

(8) Albijanic, B.; Bradshaw, D. J.; Nguyen, A. V. The relationships between the bubble−particle attachment time, collector dosage and the mineralogy of a copper sulfide ore. *Miner. Eng.* **2012**, *36-38*, 309−313.

(9) Zawala, J.; Kosior, D. Dynamics of dewetting and bubble attachment to rough hydrophobic surfaces−Measurements and modelling. *Miner. Eng.* **2016**, *85*, 112−122.

(10) Chen, S.; Yang, Z.; Chen, L.; Tao, X.; Tang, L.; He, H. Wetting thermodynamics of low rank coal and attachment in flotation. *Fuel* **2017**, *207*, 214−225.

(11) Nguyen, A. V.; Schulze, H. J. *Colloidal science of flotation*. *118*, CRC Press.

(12) Drelich, J. W.; Bowen, P. K. Hydrophobic nano-asperities in control of energy barrier during particle-surface interactions. *Surf. Innovations* **2015**, *3*, 164−171.

(13) Nguyen, A. V. One-step analysis of bubble-particle capture interaction in dissolved-air flotation. *Int. J. Environ. Pollut.* **2007**, *30*, 231−253.

(14) Gu, G.; Xu, Z.; Nandakumar, K.; Masliyah, J. Effects of physical environment on induction time of air-bitumen attachment. *Int. J. Miner. Process.* **2003**, *69*, 235−250.

(15) Peng, F. F. Surface energy and induction time of fine coals treated with various levels of dispersed collector and their correlation to flotation responses. *Energy Fuels* **1996**, *10*, 1202−1207.

(16) Wang, J.; Xie, L.; Zhang, H.; Liu, Q.; Liu, Q.; Zeng, H. Probing interactions between sphalerite and hydrophobic/hydrophilic surfaces: Effect of water chemistry. *Powder Technol.* **2017**, *320*, 511−518.

(17) Englert, A. H.; Krasowska, M.; Fornasiero, D.; Ralston, J.; Rubio, J. Interaction force between an air bubble and a hydrophilic spherical particle in water, measured by the colloid probe technique. *Int. J. Miner. Process.* **2009**, *92*, 121−127.

(18) Shi, C.; Cui, X.; Xie, L.; Liu, Q.; Chan, D. Y. C.; Israelachvili, J. N.; Zeng, H. Measuring forces and spatiotemporal evolution of thin water films between an air bubble and solid surfaces of different hydrophobicity. *Acs Nano* **2015**, *9*, 95−104.

(19) Xing, Y.; Xu, X.; Gui, X.; Cao, Y.; Xu, M. Effect of kaolinite and montmorillonite on fine coal flotation. *Fuel* **2017**, *195*, 284−289.

(20) Wang, W.; Zhou, Z.; Nandakumar, K.; Xu, Z.; Masliyah, J. H. Attachment of individual particles to a stationary air bubble in model systems. *Int. J. Miner. Process.* **2003**, *68*, 47−69.

(21) Zhuo, Q.; Liu, W.; Xu, H.; Sun, X.; Zhang, H.; Liu, W. The effect of collision angle on the collision and attachment behavior of coal particles and bubbles. *Processes.* **2018**, *6*, 218.
(22) Kouachi, S.; Vaziri, H. B.; Hassanzadeh, A.; Çelik, M. S.; Bouhenguel, M. Effect of Negative Inertial Forces on Bubble-Particle Collision via Implementation of Schulze Collision Efficiency in General Flotation Rate Constant Equation. *Colloids Surf., A* **2017**, *517*, 72−83.
(23) Karakas, F.; Hassas, B. V. Effect of Surface Roughness on Interaction of Particles in Flotation. *Physicochem. Probl. Miner. Process.* *52*.
(24) Verrelli, D. I.; Bruckard, W. J.; Koh, P. L. Particle shape effects in flotation. Part 1: Microscale experimental observations. *Miner. Eng.* **2014**, *58*, 80−89.
(25) Zhuo, Q.; Liu, W.; Xu, H. Research progress of relative motion between particles and bubbles in froth flotation. *Journal of China Coal Society* **2019**, *44*, 2867−2877.
(26) Ireland, P. M.; Jameson, G. J. Collision of a rising bubble-particle aggregate with a gas−liquid interface. *Int. J. Miner. Process.* **2014**, *130*, 1−7.
(27) Lecrivain, G.; Petruccoi, G.; Rudolph, M.; Hampel, U.; Yamamoto, R. Attachment of solid elongated particles on the surface of a stationary gas bubble. *Int. J. Multiphase Flow* **2015**, *71*, 83−93.
(28) Hassas, B. V.; Caliskan, H.; Guven, O.; Karakas, F.; Cinar, M.; Celik, M. S. Effect of roughness and shape factor on flotation characteristics of glass beads. *Colloids Surf., A* **2016**, *492*, 88−99.
(29) Nguyen, A. V.; Evans, G. M. Movement of fine particles on an air bubble surface studied using high-speed video microscopy. *J. Colloid Interface Sci.* **2004**, *273*, 271−277.
(30) Li, S.; Schwarz, M. P.; Yang, W.; Feng, Y.; Witt, P.; Sun, C. Experimental observations of bubble-particle collisional interaction relevant to froth flotation, and calculation of the associated forces. *Miner. Eng.* **2020**, *151*, 106335.
(31) Zhuo, Q.; Liu, W.; Liu, W.; Kai, P. Experimental study on the attachment behavior of coal particles and bubbles. *J. Chin. Coal Soc.* **2018**, *43*, 2029−2035.
(32) Krasowska, M.; Malysa, K. Wetting films in attachment of the colliding bubble. *Adv. Colloid Interface Sci.* **2007**, *134-135*, 138−150.
(33) Zhuo, Q.; Liu, W.; Zhang, H.; Zhang, W.; Cui, R. Effect of particle size on the relative motion between particles and bubbles. *Colloids Surf., A* **2020**, *601*, 124956.
(34) Preuss, M.; Butt, H. J. Direct Measurement of particle bubble interactions in aqueous electrolyte: dependence on surfactant. *Langmuir* **1998**, *14*, 3164−3174.
(35) Ye, Y.; Miller, J. D. Bubble Particle Contact Time in the Analysis of Coal Flotation. *Coal Prep.* **1988**, *5*, 147−166.
(36) Xing, Y.; Gui, X.; Cao, Y. The hydrophobic force for bubble particle attachment in flotation-a brief review. *Phys. Chem. Chem. Phys.* **2017**, *19*, 24421−24435.
(37) Wang, W.; Zhou, Z.; Nandakumar, K.; Xu, Z.; Masliyah, J. H. Effect of surface mobility on the particle sliding along a bubble or a solid sphere. *J. Colloid Interface Sci.* **2003**, *259*, 81−88.

https://doi.org/10.1021/acsomega.0c04093
ACS Omega 2021, 6, 7979−7987